



ELSEVIER

Contents lists available at ScienceDirect

Linear Algebra and its Applications

journal homepage: www.elsevier.com/locate/laa

Minimizing the Kohn–Sham total energy for periodic systems

Chao Yang*, Juan C. Meza

Computational Research Division, Lawrence Berkeley National Laboratory, 1 Cyclotron Road, Berkeley, CA 94720, USA

ARTICLE INFO

Article history:

Available online xxx

Submitted by V. Mehrmann

Keywords:

Kohn–Sham equations

Eigenvalues

Constrained minimization

Bloch theorem

Circulant matrices

Discrete Fourier transform

Periodic system

ABSTRACT

We describe how a previously developed constrained minimization algorithm can be adapted to minimize the total energy of a periodic atomistic system under the Kohn–Sham density functional theory framework. The algorithm uses the Bloch theorem to reduce the complexity of the calculation by working with a number of unit cells separately. We present the Bloch theorem in terms of linear algebra, and point out its implication on the spectral property of the Kohn–Sham Hamiltonian.

© 2011 Elsevier Inc. All rights reserved.

1. Introduction

A widely used methodology for studying the electronic structures of molecules and solids is to solve the Kohn–Sham problem [1], which can be formulated as either a constrained minimization problem or a nonlinear eigenvalue problem. The objective function to be minimized is the Kohn–Sham total energy functional expressed by

$$E_{\text{total}}^{\text{KS}} = \frac{1}{2} \sum_{i=1}^{n_e} \int_{\Omega} |\nabla \psi_i(r)|^2 dr + \int_{\Omega} \rho(r) V_{\text{ion}}(r) dr + \frac{1}{2} \int_{\Omega} \int_{\Omega} \frac{\rho(r) \rho(r')}{|r - r'|} dr dr' + E_{\text{xc}}(\rho), \quad (1)$$

where ψ_i ($i = 1, 2, \dots, n_e$) are called the *single-particle* wavefunctions that satisfy the orthonormality constraint $\int_{\Omega} \psi_i^* \psi_j = \delta_{i,j}$, n_e corresponds to the number of electrons in the system and $\Omega \subset \mathbb{R}^3$. The *charge density* $\rho(r)$, which gives the probability density of finding an electron at $r \in \mathbb{R}^3$ is defined by

$$\rho(r) = \sum_{i=1}^{n_e} \psi_i^*(r) \psi_i(r). \quad (2)$$

* Corresponding author.

E-mail address: cyang@lbl.gov (C. Yang).

The function $V_{ion}(r) = \sum_{j=1}^{n_u} z_j/|r - \hat{r}_j|$ represents the ionic potential induced by n_u nuclei with positive charges z_j ($j = 1, 2, \dots, n_u$), and $E_{xc}(\rho)$ is known as the exchange–correlation energy, which accounts for the many-body effects of the electrons [2].

For the purpose of this paper, we are not concerned with the analytic expression of $E_{xc}(\rho)$ other than the assumption that E_{xc} depends only on ρ . This assumption is based on what is known as the local density approximation (LDA) [1].

It is not difficult to show that the first order necessary condition (Euler–Lagrange equation) for the constrained minimization problem

$$\begin{aligned} \min \quad & E_{total}^{KS}(\{\psi_i\}) \\ \{\psi_i\} \quad & \\ \text{s.t.} \quad & \psi_i^* \psi_j = \delta_{i,j} \end{aligned} \quad (3)$$

has the form

$$H(\rho)\psi_i = \lambda_i\psi_i, \quad i = 1, 2, \dots, n_e, \quad (4)$$

$$\psi_i^* \psi_j = \delta_{i,j}. \quad (5)$$

where the single-particle Hamiltonian $H(\rho)$ (also known as the Kohn–Sham Hamiltonian) is defined by

$$H(\rho) = -\frac{1}{2}\Delta + V_{ion}(r) + \int_{\Omega} \frac{\rho(r')}{|r - r'|} dr' + V_{xc}(\rho(r)). \quad (6)$$

The function $V_{xc}(\rho)$ in (6) is the functional derivative of $E_{xc}(\rho)$ with respect to ρ . The ionic potential V_{ion} can be replaced by what is called *ionic pseudopotential* to account for the net effect of nuclei and inner electrons in completely filled electron orbitals [3–5]. In this case, $\psi_i, i = 1, 2, \dots, n_e$, will simply correspond to n_e valence electrons. For the rest of this paper, we define

$$V_{ext}(\rho(r)) = V_{ion}(r) + \int_{\Omega} \frac{\rho(r')}{|r - r'|} dr' + V_{xc}(\rho(r)),$$

and will not be concerned with the calculation details associated with each individual term in $V_{ext}(\rho(r))$.

Because the Kohn–Sham Hamiltonian is a function of ρ , which is in turn a function of $\{\psi_i\}$, the set of equations defined by (4) results in a nonlinear eigenvalue problem. These equations are collectively referred to as the *Kohn–Sham equations*. Interested readers can learn more about these equations from several sources (e.g., [6]).

In this paper, we are concerned with solving the Kohn–Sham problem for periodic systems such as crystalline solids. These systems are characterized by periodic extensions of a unit cell in 3D, where each unit cell contains a number of atoms. The relative positions of these atoms within the cell are periodically extended also. As a result, both the charge density $\rho(r)$ and the potential $V_{ext}(r)$ are periodic functions. It is tempting to believe that the single particle functions $\{\psi_i\}$ ($i = 1, 2, \dots, n_e$) that satisfy (4) are also periodic. But they are not. However, they have a special structure that is characterized by what is known as the *Bloch theorem* [7–9]. Because of this structure, the task of solving the Kohn–Sham problem for the entire periodic system can be reduced to that involving only the unit cell. We will state the Bloch theorem in the next section and explain the implication of this theorem on the spectral property of the discretized Kohn–Sham Hamiltonian using linear algebra. We will show how this theorem can be used to reduced the complexity of solving the Kohn–Sham problem for periodic systems. We will focus on one particular algorithm we developed in [10], and show that it can be easily modified to efficiently minimize the Kohn–Sham total energy for a periodic system.

Standard linear algebra notation is used for vectors and matrices throughout the paper. We use $\text{Diag}(v)$ to denote a diagonal matrix with the vector v on its diagonal. Similarly, we use $\text{diag}(V)$ to denote a vector that consists of the diagonal elements of the matrix V . If $A^{(k)}$, $k = 0, 1, \dots, p-1$, are $m \times m$ matrices, then we use $\text{Diag}(A^{(0)}, A^{(1)}, A^{(p-1)})$ to denote a $pm \times pm$ block diagonal matrix that contains p diagonal blocks $A^{(k)}$, $k = 0, 1, \dots, p-1$. We define $\omega_n^k = e^{i2\pi k/n}$. If k divides n , then $\omega_n^k = \omega_{n/k}$.

2. Bloch theorem

For simplicity, we will first restrict ourselves to a 1D Schrödinger type of operator of the form

$$H = \frac{d^2}{dr^2} + V(r), \quad (7)$$

defined on an open domain $\Omega = (-\infty, \infty)$, where $V(x)$ is periodic with a period R . The Bloch theorem states that the eigenfunction $\psi(r)$ of H can be expressed by

$$\psi(r) = e^{ik(2\pi/R)r} u^{(k)}(r), \quad (8)$$

where $u^{(k)}(r)$ is R -periodic, i.e., $u^{(k)}(r+R) = u^{(k)}(r)$. To account for the k dependency of $\psi(r)$, we introduce a subscript k in $\psi(r)$ and denote it by $\psi_k(r)$. When $\Omega = (-\infty, \infty)$, the operator defined in (7) has a infinite number of eigenfunctions because $k \in \mathbb{R}$. However, in practice, the open domain is often truncated to make the task of computing the eigenpairs of H numerically tractable. One way to restrict the domain is to impose an additional periodic boundary condition of the form

$$\psi(r) = \psi(r+pR), \quad (9)$$

where $p > 0$ is an integer. The boundary condition defined by (9) is often known as the *Born-von Karman* boundary condition [8].

It is a simple exercise to show that (8) and (9) imply that the allowed k values in (8) must satisfy

$$k = \frac{\tilde{k}}{p}, \quad (10)$$

where \tilde{k} is an integer. Furthermore, because $u^{(k)}(r)$ is periodic, we only need to consider \tilde{k} in the interval $[0, p-1]$. The values of $2\pi k/R$, where k is defined by (10) are often referred to as k -points in solid state physics. The interval $[0, 2\pi/R)$ is known as the *first Brillouin Zone* (BZ). (The choice of a BZ is not unique. For example, $[-\pi/R, \pi/R)$ is also a valid BZ.) Clearly, the number of allowed k -points depends on the value of p .

The distance between two adjacent k -points depends on both p and R . As p approaches infinity (which is referred to as the bulk limit in solid-state physics), the set of k -points forms a continuum in $[0, 2\pi/R)$. When R (which is referred to as the unit cell size in solid-state physics) is sufficient large, $2\pi/R$ becomes very small so that the variation among different k -points is negligible. In this case, it is sufficient to consider one k -point (e.g., the one associated with $k = 0$) when eigenpairs of H are computed.

The standard proof of the Bloch theorem utilizes the fact that H commutes with the translation operator \mathcal{T} defined as

$$\mathcal{T}f = f(r-R),$$

for any function f [8,9]. In the following, we present a simpler interpretation of the theorem using matrix notation. This interpretation is useful for analyzing the spectral properties of a finite dimension

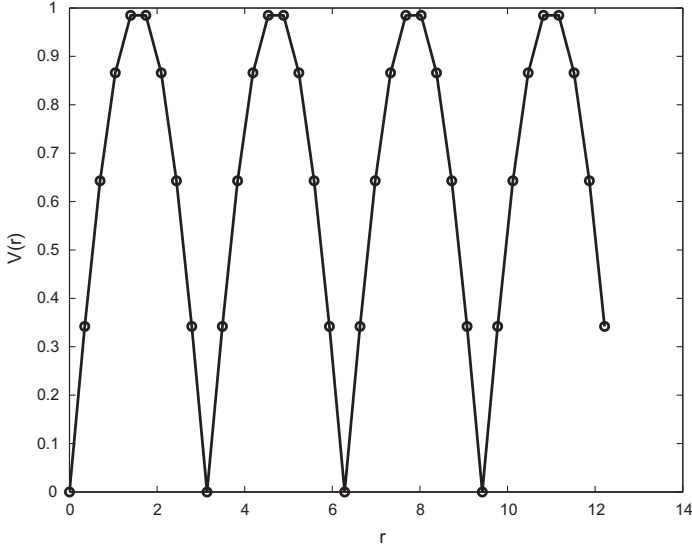


Fig. 1. A discretized periodic potential defined on $[0, 4\pi)$ with period $R = \pi$. The number of periods shown here is $p = 4$ and the number of sampling points in each unit cell is $m = 9$.

problem obtained from a discretization of H on a bounded domain. Unless otherwise noted, the Born–von Karman boundary condition of the form (9) is imposed.

For simplicity, let us assume that d^2/dr^2 is discretized by central differences to yield a circulant matrix of the form

$$T = \begin{pmatrix} 2 & -1 & & -1 \\ -1 & 2 & \ddots & \\ & \ddots & \ddots & -1 \\ -1 & & -1 & 2 \end{pmatrix}. \quad (11)$$

The unit cell $[0, R)$ is sampled uniformly by m points $r_j = (j-1)R/m, j = 0, 1, \dots, m-1$. As a result, the dimension of T is $n = mp$, and the discretized $V(r)$ in (7) is a diagonal matrix with a periodically replicated vector v on its diagonal. Fig. 1 shows a discretized periodic potential function for $m = 9$, $p = 4$ and $R = \pi$.

Because T is a circulant matrix, it can be diagonalized by the discrete Fourier transform matrix F_n , where the (k, j) th entry is defined by $F_n(j, k) = e^{i(2\pi/n)kj}/\sqrt{n}, j, k = 0, 1, \dots, n-1$ [11]. With this matrix F_n , we can decompose T as

$$T = F_n D F_n^*, \quad (12)$$

where D is a diagonal matrix. If we denote the diagonal of D by $d = \text{diag}(D)$, then it is well known that $d = F_n T e_1$, i.e., the eigenvalues of T are simply the elements of the discrete Fourier transform of the first column of T .

Using (12), we can rewrite H as

$$H = T + V = F_n (D + F_n^* V F_n) F_n^* \quad (13)$$

Because V is diagonal, the $F_n^* V F_n$ term in (13) is a circulant matrix. The first column of this matrix can be constructed by taking the discrete Fourier transform of the diagonal of V . Subsequent columns can

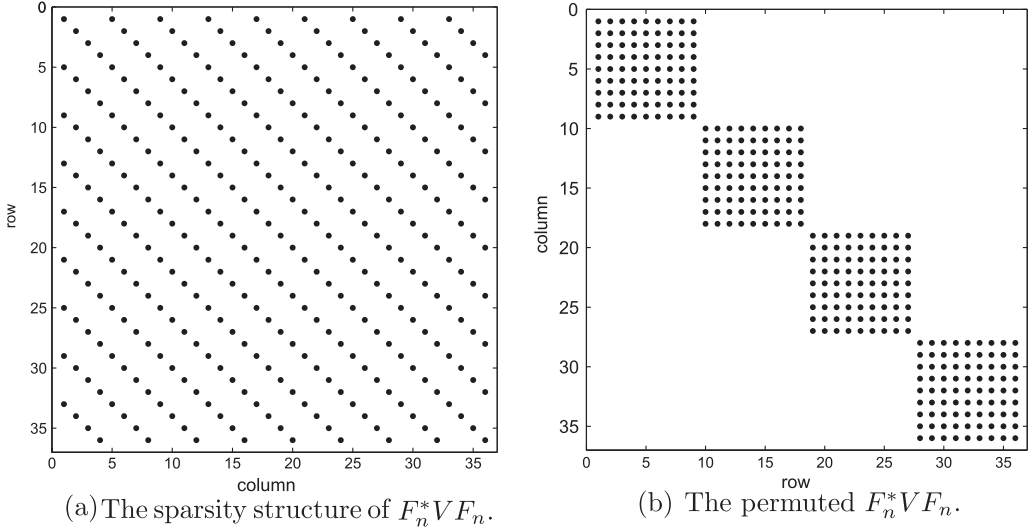


Fig. 2. The sparsity of $F_n^* V F_n$ before and after it is permuted.

be formed by circularly shifting the first column incrementally. Furthermore, because the $v = \text{diag}(V)$ contains p periods of a uniformly sampled potential function, the inverse discrete Fourier transform of v is non-zero every p points. That is, if $f = F_n^* v$, then $e_j^T f \neq 0$ only when $j = p\ell$, $\ell = 0, 1, \dots, m-1$. Consequently, the matrix $F_n^* V F_n$ is sparse with $m-1$ strips in the lower (and the upper) triangular part of the matrix as shown in Fig. 2.

It is easy to verify that $F_n^* V F_n$ can be permuted into a block diagonal matrix with p diagonal blocks. Fig. 2 depicts the resulting permuted matrix for this example. Let P be the permutation matrix that achieves this task, i.e., P makes $P^T F_n^* V F_n P$ block diagonal. Then we can rewrite (7) as

$$H = F_n P \left(P^T D P + P^T F_n^* V F_n P \right) P^T F_n^*. \quad (14)$$

Because D is a diagonal matrix, $P^T D P$ remains a diagonal matrix. Consequently, the matrix

$$G = P^T D P + P^T F_n^* V F_n P, \quad (15)$$

is also block diagonal. Because G is obtained from H through a unitary transformation $F_n P$, computing the eigenvalues of H is equivalent to computing the eigenvalues of each diagonal block in G .

Suppose $\hat{u}^{(k)}$ is an eigenvector of the k th diagonal block of G , then the vector

$$z = F_n P E_k \hat{u}^{(k)},$$

is an eigenvector of H , where the $n \times m$ matrix $E_k = (0 \ \cdots \ I_m \ 0)^T$ contains the $m \times m$ identity matrix I_m between rows $km+1$ and $(k+1)m$ and zero everywhere else. That is, E_k simply picks out columns $(k-1)m+1$ through km of the matrix $F_n P$. It is easy to show that $F_n P E_k$ can be expressed as

$$F_n P E_k = \Omega_k \begin{pmatrix} F_m \\ F_m \\ \vdots \\ F_m \end{pmatrix}, \quad (16)$$

where $\Omega_k = \text{Diag} \left(1, \omega_n^k, \omega_n^{2k}, \dots, \omega_n^{(n-1)k} \right)$ and $\omega_n = e^{i2\pi/n}$. It follows that

$$z = F_n P E_k \hat{u}^{(k)} = \Omega_k \begin{pmatrix} F_m \hat{u}^{(k)} \\ F_m \hat{u}^{(k)} \\ \vdots \\ F_m \hat{u}^{(k)} \end{pmatrix}.$$

This is precisely what is stated in the Bloch theorem. That is, the j th element of an eigenvector z of H can be expressed as

$$\begin{aligned} e_j^T z &= \omega_n^{k(j-1)} e_j^T F_m \hat{u}^{(k)}, \\ &= e^{i2\pi k(j-1)/n} u^{(k)}(r_j) \\ &= e^{i(2\pi/R)(k/p)[(j-1)(pR)/n]} u^{(k)}(r_j) \\ &= e^{i(2\pi/R)\tilde{k}r_j} u^{(k)}(r_j) \end{aligned} \quad (17)$$

where we have used the definition $r_j = (j-1)(pR)/n$, $\tilde{k} = k/p$ and $u^{(k)} = F_m \hat{u}^{(k)}$ is periodic with the period R .

The Bloch theorem suggests the eigenvalues of a matrix Hamiltonian that contains a periodic potential with p periods can be computed by solving p smaller eigenvalue problems defined on p unit cells. Each unit cell corresponds to an $m \times m$ diagonal block of the G matrix defined in (15). We denote the k th diagonal block of G by $G^{(k)}$ where $k = 0, 1, 2, \dots, p-1$ and label the eigenvalues of $G^{(k)}$ by

$$\lambda_1^{(k)} \leq \lambda_2^{(k)} \leq \dots \leq \lambda_m^{(k)}.$$

The eigenvectors associated with these eigenvalues are indexed as $z_1^{(k)}, z_2^{(k)}, \dots, z_m^{(k)}$, for $k = 0, 1, \dots, p-1$. The set of eigenvalues $\mathcal{B}_j = \{\lambda_j^{(0)}, \lambda_j^{(1)}, \dots, \lambda_j^{(p-1)}\}$ is said to form the j th energy band in solid-state physics. As p approaches infinity (the bulk limit), the plot of eigenvalues in \mathcal{B}_j against the k points forms a continuous curve. The set of curves $\{\mathcal{B}_j\}$ gives what is known as the *band-structure* of the (solid) material associated with the Hamiltonian H . Fig. 3 shows the band structure of the artificial material associated with the Hamiltonian defined by the potential shown in Fig. 1.

We should also note that the eigenvalue problems associated with different diagonal block of G are not completely independent from each other. In particular, it follows from periodicity of V that all diagonal blocks of the second term $P^T F_n^* V F_n P$ in (15) are identical. Because they are all circulant, they can all be diagonalized by F_m , i.e., we may express $P^T F_n^* V F_n P$ as

$$P^T F_n^* V F_n P = \text{Diag} \left(F_m^* \hat{V} F_m, F_m^* \hat{V} F_m, \dots, F_m^* \hat{V} F_m \right),$$

where \hat{V} is an $m \times m$ diagonal matrix, whose diagonal elements are simply $V(r_j)$ for $r_j = (R/m)j$, $j = 0, 1, 2, \dots, m-1$.

If the first term $P^T D P$ of (15) is partitioned conformally with the second term, i.e.,

$$P^T D P = \text{Diag} \left(D^{(0)}, D^{(1)}, \dots, D^{(p-1)} \right),$$

then we can rewrite G as

$$G = \text{Diag} \left(F_m^* \hat{H}^{(0)} F_m, F_m^* \hat{H}^{(1)} F_m, \dots, F_m^* \hat{H}^{(p-1)} F_m \right) \quad (18)$$

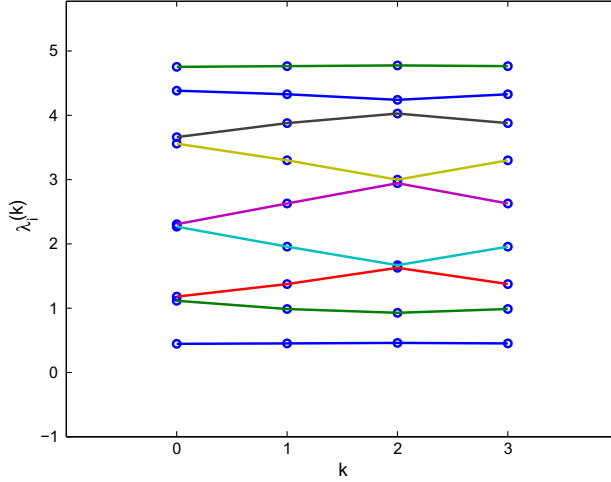


Fig. 3. The band structure eigenvalue plot for the discretized $H = T + V$, where the potential function V is defined as in Fig. 1.

where $\hat{H}^{(k)} = F_m D^{(k)} F_m^* + \hat{V}$ for $k = 0, 1, \dots, p-1$. Again, because $D^{(k)}$ is diagonal, the matrix $F_m D^{(k)} F_m^*$ must be circulant with its first column determined by the discrete Fourier transform of $d^{(k)} = \text{diag}(D^{(k)})$. Because $d^{(k)}$ is uniformly down-sampled from every p th entry of $d = F T e_1$, $F_m d^{(k)}$ can be obtained by truncating $T e_1$ and multiplying the off-diagonal entries by appropriate phase factors to account for the shifting in the starting point of the subsamples contained in $d^{(k)}$. (See Appendix for details.) As a result, we can rewrite $\hat{H}^{(k)}$ as

$$\hat{H}^{(k)} = \hat{T}^{(k)} + \hat{V}, \quad (19)$$

where the $m \times m$ matrix

$$\hat{T}^{(k)} = \begin{pmatrix} 2 & \omega_n^{-k} & & \omega_n^k \\ \omega_n^k & 2 & \ddots & \\ & \ddots & \ddots & \omega_n^{-k} \\ \omega_n^{-k} & & \omega_n^k & 2 \end{pmatrix} \quad (20)$$

has the same sparsity structure as that of (11), but with $1/p$ th of its dimension. If $u^{(k)}$ is an eigenvector of $H^{(k)}$, it follows from (18) that $u^{(k)} = F_m \hat{u}^{(k)}$.

To see more clearly how $\hat{H}^{(k)}$'s, $k = 0, 1, 2, \dots, p-1$, are related to H , we can rewrite $F_n P E_k$ as

$$F_n P E_k = \Omega_k \begin{pmatrix} F_m \\ F_m \\ \vdots \\ F_m \end{pmatrix} = \begin{pmatrix} \hat{\Omega}_k \\ \omega_n^{km} \hat{\Omega}_k \\ \vdots \\ \omega_n^{(p-1)km} \hat{\Omega}_k \end{pmatrix} F_m = \begin{pmatrix} \hat{\Omega}_k \\ \omega_p^k \hat{\Omega}_k \\ \vdots \\ \omega_p^{k(p-1)} \hat{\Omega}_k \end{pmatrix} F_m$$

where $\hat{\Omega}_k = \text{Diag}(1, \omega_n^k, \omega_n^{2k}, \dots, \omega_n^{(m-1)k})$. Therefore, we have

$$F_n P = W \text{Diag}(F_m, F_m, \dots, F_m), \quad (21)$$

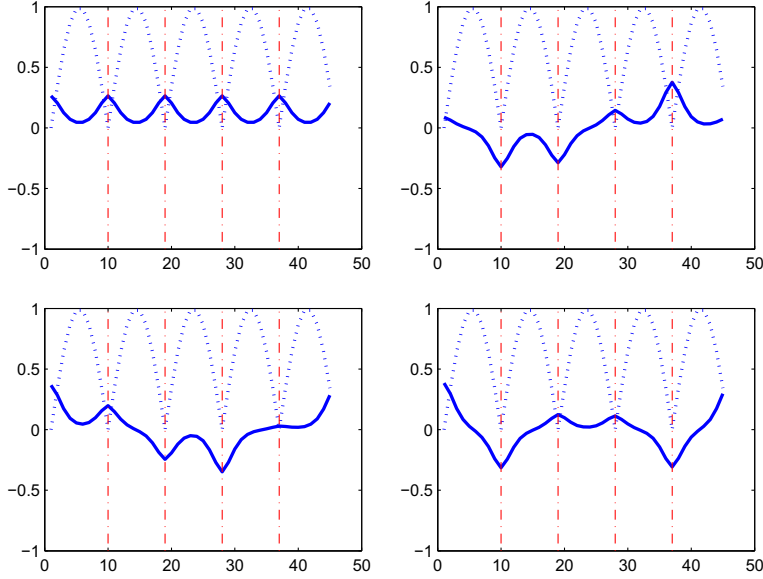


Fig. 4. The eigenvectors associated with the four smallest eigenvalues of $H = T + V$, where the potential function V is defined as in Fig. 1. In addition to the eigenvectors which are shown in solid curves, we also plot the periodic potential in each sub-figure using dotted curves. The separation of different periods are marked vertical dash-dotted lines.

where

$$W = \begin{pmatrix} \hat{\Omega}_0 & \hat{\Omega}_1 & \cdots & \hat{\Omega}_{p-1} \\ \hat{\Omega}_0 & \omega_p \hat{\Omega}_1 & \cdots & \omega_p^{p-1} \hat{\Omega}_{p-1} \\ \vdots & \vdots & \ddots & \vdots \\ \hat{\Omega}_0 & \omega_p^{p-1} \hat{\Omega}_1 & \cdots & \omega_p^{(p-1)^2} \hat{\Omega}_{p-1} \end{pmatrix}. \quad (22)$$

It follows from (14), (18) and (21) that

$$H = W \begin{pmatrix} \hat{H}^{(0)} & & & \\ & \hat{H}^{(1)} & & \\ & & \ddots & \\ & & & \hat{H}^{(p-1)} \end{pmatrix} W^*. \quad (23)$$

It is easy to verify that W , which can be permuted into a block diagonal matrix, is unitary. Therefore, the Bloch theorem allows us to compute the eigenpairs of H defined for a periodic system by focusing on a number of unit cell eigenvalue problems which are much smaller in dimension compared to the entire domain that consists of several unit cells. The Hamiltonians associated with different unit cell eigenvalue problems differ only in their kinetic energy operators. The solutions to the unit cell problems are ultimately coupled (modulated) by the W matrix defined by (22). Fig. 4 shows how the four eigenvectors associated with the four smallest eigenvalues of H (which forms the first energy band) look like.

We should point out that the exact form of the discretized kinetic energy operator $\hat{T}^{(k)}$ depends on how d^2/dr is discretized. Regardless of how it is discretized, it should contain a “phase factor”

modification that depends on k . For example, if a plane wave (or truncated Fourier series) expansion is used to discretize d^2/dr , then $\hat{T}^{(k)}$ can be represented by

$$\hat{T}^{(k)} = F_m \text{Diag} \left(\sigma_1^{(k)}, \sigma_2^{(k)}, \dots, \sigma_m^{(k)} \right) F_m^*, \quad (24)$$

where $\sigma_j^{(k)} = |(2\pi/m)(j-1)(1+k/p)|^2$.

Although we have used a 1D example to illustrate the implication of the Bloch theorem, all the results above can be easily extended to 2D and 3D problems. For a 2D or 3D problem, the discretized kinetic energy operator has a block circulant structure with circulant matrix blocks. This type of matrix as well as the discretized Fourier transformation matrix F_n can be represented as a Kronecker product of lower dimensional matrices.

3. Constrained minimization for Kohn–Sham energy

It is reasonable to assume that the electron density for a periodic system is periodic at the minimum energy state, i.e., electrons are distributed in the same way from one unit cell to another. Hence, the Kohn–Sham Hamiltonian defined by (6) contains a periodic potential $V_{\text{ext}}(r)$. As a result, the solution to the Kohn–Sham problem, which consists of a set of eigenfunctions of $H(\rho)$, must satisfy the Bloch theorem, i.e., each eigenfunction can be expressed by $\psi_k(r) = e^{ik(2\pi/R)r} u^{(k)}(r)$, where $u^{(k)}(r)$ is R -periodic.

After H is discretized, the total number of eigenvectors associated with the discretized H is $n = mp$, where m is the number of degrees of freedom per unit cell introduced by the discretization (e.g., the number of grid points in the finite difference discretization or the number of planewaves used in a planewave discretization) and p is the number of unit cells included in the finite dimensional approximation. As we pointed out earlier, these eigenvectors can be labeled as $z_1^{(k)}, z_2^{(k)}, \dots, z_m^{(k)}$. Such a double-index labeling must be taken into account in the charge density computation described by (2). Although it has not been rigorously proved, it is generally accepted that the charge density associated with the minimum Kohn–Sham energy should obey the *aufbau principle* [12] at zero temperature, i.e., the n_e eigenfunctions that are included in the summation (2) must be those that are associated with the n_e smallest eigenvalues of H . These eigenvalues should not be larger than what is called the *Fermi level* or chemical potential denoted by ϵ_F .

It is well known in solid-state physics that for insulator and semiconductors, the smallest n_e eigenvalues H tend to fill the lowest few energy bands that are separated from higher energy bands by a measurable distance (or gap), i.e., the smallest n_e eigenvalues of H are precisely those in $\cup_{\ell=1}^s \mathcal{B}_\ell$, where $\mathcal{B}_\ell = \{\lambda_\ell^{(0)}, \lambda_\ell^{(1)}, \dots, \lambda_\ell^{(p-1)}\}$, and $n_e = ps$. As a result, we may rewrite (2) as

$$\rho = \sum_{k=0}^{p-1} \sum_{\ell=1}^s |z_\ell^{(k)}|^2 = \left(\hat{\rho}^T \quad \hat{\rho}^T \quad \dots \quad \hat{\rho}^T \right)^T, \quad (25)$$

where $\hat{\rho} = \sum_{k=0}^{p-1} \sum_{\ell=1}^s |u_\ell^{(k)}|^2$ and $u_\ell^{(k)}$ is the eigenvector corresponding to the ℓ th smallest eigenvalue of the unit cell Hamiltonian $\hat{H}^{(k)}$ defined by (19). Note that ρ is the overall charge density associated with the atomistic system that contains p unit cells. The expression on the right-hand side of (25) indicates that it is periodic with p periods. Within each unit cell, the charge density is given by $\hat{\rho}$. The phase factor $\omega_n^{k(j-1)}$ that appears in the j th element of the eigenvector $z_\ell^{(k)}$, as shown in (17), does not enter the charge density ($\hat{\rho}$) calculation because it cancels with its conjugate.

For metallic systems in which the lowest energy bands may be partially filled, expression (25) does not hold in general. That is, the ℓ th eigenvalue associated with one particular k -point may be smaller than the $\ell - j$ th eigenvalue associated with a different k -point for some integer j . However, to simplify our discussion below, we will not be concerned with this case, and we will use (25) as the definition of charge density.

We should also comment that as p approaches infinity, the summation over k is replaced by integration over $k \in \mathbb{R}^d$ ($d = 1, 2$ or 3) in the first BZ. The integration can be approximated by an appropriate quadrature rule. In solid-state physics, efficient and accurate quadrature rules that take advantage of crystal symmetry are often used [13]. These quadrature rules result in special k -points that are different from the evenly space k -points that result from the use of the Born–von Karman boundary condition.

We will show in the following how the direct constrained minimization (DCM) algorithm we introduced in [10, 14] can be used to minimize the Kohn–Sham total energy for periodic systems. Our objective here is not to introduce a new optimization algorithm but merely to illustrate how the Bloch theorem is used to modify DCM so that it can be used on periodic systems.

We assume that the Kohn–Sham minimization problem (1) has been discretized. What we will show below is applicable to different discretization schemes. However, the most natural discretization scheme for periodic system is the planewave discretization. The finite-dimensional Kohn–Sham minimization problem can be stated as

$$\min_{X^*X=I_{n_e}} \text{trace}(X^*H(\rho(X))X), \quad (26)$$

where the finite-dimensional Kohn–Sham Hamiltonian can be written as

$$H(\rho(X)) = \frac{1}{2}L + V_{\text{ext}}(\rho(X)),$$

and $\rho(X) = \text{diag}(XX^*)$ is the discretized version of $\rho(r)$ defined in (25). Here L is the matrix representation of the discretized Laplacian or kinetic energy operator.

It follows from the discussion in the previous section that we can express a finite-dimensional approximation to the solution of the Kohn–Sham problem defined on a periodic system by

$$X = F_n P \text{Diag}(F_m^*, F_m^*, \dots, F_m^*) U = WU, \quad (27)$$

where $U = \text{Diag}(\hat{U}^{(0)}, \hat{U}^{(1)}, \dots, \hat{U}^{(p-1)})$ and $\hat{U}^{(k)} = (u_1^{(k)} \ u_2^{(k)} \ \dots \ u_s^{(k)})$. Here we have used the assumption that the smallest n_e eigenvalues of H fill up the lowest s energy bands and $sp = n_e$.

The basic idea of DCM is to minimize the total energy within a sequence of subspaces spanned by columns of

$$Y = (X^{(i)}, M^{-1}R^{(i)}, P^{(i-1)}), \quad (28)$$

where $X^{(i)} \in \mathbb{C}^{n \times n_e}$ is the approximation to X obtained at the i th iteration, $R^{(i)} = [I - X^{(i)}(X^{(i)})^*]H^{(i)}X^{(i)}$ is the projected gradient of the Kohn–Sham total energy along the tangent of the orthonormality constraint, the preconditioner M is a Hermitian positive definite preconditioner, and $P^{(i-1)}$ is the search direction obtained in the previous iteration. It was shown in [10] that solving the subspace minimization problem is equivalent to computing the eigenvectors G associated with the n_e smallest eigenvalues of the following nonlinear eigenvalue problem

$$\tilde{H}(G)G = BG\Omega, \quad G^*BG = I, \quad (29)$$

where

$$\tilde{H}(G) = Y^* \left[\frac{1}{2}L + V(\rho(YG)) \right] Y, \quad (30)$$

and $B = Y^*Y$. Because the dimension of $\tilde{H}(G)$ is $3n_e \times 3n_e$, which is normally much smaller than that of $H(X)$, it is relatively easy to solve (29) by, for example, a trust region enabled SCF (TRSCF) iteration [14]. We should note that it is not necessary to solve (29) to full accuracy in the early stage of the DCM algorithm because all we need is a G that yields sufficient reduction in the objective function.

Once G is obtained, we can update the wave function by

$$X^{(i+1)} \leftarrow YG.$$

The search direction associated with this update is implicitly defined to be

$$P^{(i)} \equiv M^{-1}R^{(i)}G_2 + P^{(i-1)}G_3, \quad (31)$$

where G_2 and G_3 are submatrices of the G matrix

$$G = \begin{pmatrix} G_1 \\ G_2 \\ G_3 \end{pmatrix}$$

partitioned conformally with the partition of Y in (28). By solving the projected problem (29) iteratively, we obtain both the search direction (31) and an appropriate step length (represented by G) to move along this direction simultaneously.

A complete description of the constrained minimization algorithm is given in Fig. 5. We should point out that solving the projected optimization problem in Step 8 of the algorithm requires us to

Algorithm DCM: A Constrained Minimization Algorithm for Total Energy Minimization

- Input:** initial set of wave functions $X^{(0)} \in \mathbb{C}^{n \times n_e}$; ionic pseudopotential; a preconditioner M ;
- Output:** $X \in \mathbb{C}^{n \times n_e}$ such that the Kohn-Sham total energy functional $E_{total}(X)$ is minimized and $X^*X = I_k$.
1. Orthonormalize $X^{(0)}$ such that $X^{(0)*}X^{(0)} = I_k$;
 2. for $i = 0, 1, 2, \dots$ until convergence
 3. Compute the charge density ρ ;
 4. Compute $\Theta = X^{(i)*}H^{(i)}X^{(i)}$;
 5. Compute $R = H^{(i)}X^{(i)} - X^{(i)}\Theta$;
 6. if $(i > 1)$ then
 $Y \leftarrow (X^{(i)}, M^{-1}R, P^{(i-1)})$;
 else
 $Y \leftarrow (X^{(i)}, M^{-1}R)$;
 endif
 7. $B \leftarrow Y^*Y$;
 8. Find $G = (G_1^T G_2^T)^T \in \mathbb{C}^{2n_e \times n_e}$ or $G = (G_1^T G_2^T G_3^T)^T \in \mathbb{C}^{3n_e \times n_e}$ that minimizes $E_{total}(YG)$ subject to the constraint $G^*BG = I_{n_e}$;
 9. Set $X^{(i+1)} = YG$;
 10. if $(i > 1)$ then
 $P^{(i)} \leftarrow M^{-1}RG_2 + P^{(i-1)}G_3$;
 else
 $P^{(i)} \leftarrow M^{-1}RG_2$;
 endif
 11. end for

Fig. 5. A direct constrained minimization algorithm for total energy minimization.

evaluate the projected Hamiltonian $\hat{H}(G)$ repeatedly as we search for the best G . However, since the first term of \tilde{H} does not depend on G , it can be computed and stored in advance. Only the second term of (30) needs to be updated. These updates require the charge density and the potential to be recomputed.

We will show next that, for periodic systems, the projected Hamiltonian defined by (30) has a block diagonal structure, and both the projected gradient $R^{(i)}$ and search direction $P^{(i)}$ can be computed on a number of unit cells separately.

It follows from (23) and (27) that

$$\begin{aligned} H^{(i)} X^{(i)} &= W \text{Diag} \left(\hat{H}^{(0)}, \hat{H}^{(1)}, \dots, \hat{H}^{(p-1)} \right) W^* W U \\ &= W \text{Diag} \left(\hat{H}^{(0)} \hat{U}^{(0)}, \hat{H}^{(1)} \hat{U}^{(1)}, \dots, \hat{H}^{(p-1)} \hat{U}^{(p-1)} \right). \end{aligned}$$

Furthermore, since

$$(X^{(i)})^* H^{(i)} X^{(i)} = \text{Diag} \left(\hat{\Theta}^{(0)}, \hat{\Theta}^{(1)}, \dots, \hat{\Theta}^{(p-1)} \right),$$

where $\hat{\Theta}^{(k)} = (\hat{U}^{(k)})^* \hat{H}^{(k)} \hat{U}^{(k)}$, the projected gradient $R^{(i)}$ can be expressed by

$$R^{(i)} = W \text{Diag} \left(\hat{R}^{(0)}, \hat{R}^{(1)}, \dots, \hat{R}^{(p-1)} \right),$$

where $\hat{R}^{(k)} = \hat{H}^{(k)} \hat{U}^{(k)} - \hat{U}^{(k)} \hat{\Theta}^{(k)}$, for $k = 0, 1, \dots, p-1$.

The search direction produced in the first iteration of the DCM algorithm is simply the projected gradient. Therefore, it has the form

$$P^{(1)} = W \text{Diag} \left(\hat{P}^{(0)}, \hat{P}^{(1)}, \dots, \hat{P}^{(p-1)} \right),$$

where $\hat{P}^{(k)}$ is simply $\hat{R}^{(k)}$. It is easy to see that this structure is preserved in subsequent DCM iterations, i.e., $P^{(k)}$ can be expressed as the product of W and a block diagonal matrix. As a result, the matrix Y in (28) has the form

$$Y = W \text{Diag} \left(\hat{Y}^{(0)}, \hat{Y}^{(1)}, \dots, \hat{Y}^{(p-1)} \right),$$

where $\hat{Y}^{(k)} = (\hat{U}^{(k)})^* \hat{R}^{(k)} \hat{P}^{(k)}$. Consequently,

$$\begin{aligned} \tilde{H} &= Y^* W \text{Diag} \left(\hat{H}^{(0)}, \hat{H}^{(1)}, \dots, \hat{H}^{(p-1)} \right) W^* Y \\ &= \text{Diag} \left(\Gamma^{(0)}, \Gamma^{(1)}, \dots, \Gamma^{(p-1)} \right), \end{aligned}$$

where $\Gamma^{(k)} = (\hat{Y}^{(k)})^* \hat{H}^{(k)} \hat{Y}^{(k)}$, and the solution G to the projected nonlinear eigenvalue problem (29) is also block diagonal, i.e.,

$$G = \text{Diag} \left(\hat{G}^{(0)}, \hat{G}^{(1)}, \dots, \hat{G}^{(p-1)} \right),$$

and $\hat{G}^{(k)} \in \mathbb{C}^{m \times n_e}$.

It follows from the above that for periodic systems that contain p unit cells, the Bloch theorem allows us to solve the subspace minimization problem in Step 8 of the DCM algorithm by working with p unit cells separately. These unit cells are coupled through the W matrix in the periodic charge density $\rho(YG)$, which can be represented by

$$\rho(YG) = \text{diag}(YG(YG)^*) = \begin{pmatrix} \hat{\rho}^T & \hat{\rho}^T & \dots & \hat{\rho}^T \end{pmatrix}^T$$

where $\hat{\rho} = \sum_{k=0}^{p-1} \text{diag}[\hat{Y}^{(k)} \hat{G}^{(k)} (\hat{G}^{(k)})^* (\hat{Y}^{(k)})^*]$. The projected Hamiltonians $\hat{H}^{(k)}$ defined on different unit cells differ in their kinetic energy operator $\hat{T}^{(k)}$ which must account for a phase shift such as that shown in (20). The same observation can be made by rewriting the objective function (26) as a sum of traces using

$$\begin{aligned} \text{trace}[X^* H(\rho(X)) X] &= \text{trace}[(WU)^* W \text{Diag}(\hat{H}^{(0)}, \hat{H}^{(1)}, \dots, \hat{H}^{(p-1)}) W^* WU] \\ &= \sum_{k=0}^{p-1} \text{trace}[(\hat{U}^{(k)})^* \hat{H}^{(k)} \hat{U}^{(k)}]. \end{aligned}$$

The orthonormality constraint $X^* X = I_n$ can also be replaced by p separate orthonormality constraints $(\hat{U}^{(k)})^* \hat{U}^{(k)} = I_m$, for $k = 0, 1, \dots, p-1$. Note that $\hat{H}^{(k)}$ is a function of $\hat{\rho}$ for $k = 0, 2, \dots, p-1$.

In terms of algorithmic changes, we can simply modify the DCM algorithm shown in Fig. 5 by introducing an additional loop indexed by k on unit cells inside the DCM iteration loop indexed by i . All the underlined steps in Algorithm 1 (Fig. 5) should be placed inside this inner loop. The k th iterate of this loop will take $\hat{H}^{(k)}$ and $\hat{U}^{(k)}$ (instead of $H^{(i)}$ and $X^{(i)}$) as input, and compute $\hat{\Theta}^{(k)}$, $\hat{R}^{(k)}$ and $\hat{Y}^{(k)}$ for each $k = 0, 1, \dots, p-1$. Just as in the original DCM algorithm, the subspace minimization problem that appears in Step 8 must be solved iteratively by using, for example, a trust-region enabled SCF (TRSCF) iteration [14]. Because the first order necessary condition for this constrained minimization problem yields p coupled nonlinear eigenvalue problems of form

$$\hat{H}^{(k)}(\hat{\rho}) \hat{G}^{(k)} = \hat{B}^{(k)} \hat{G}^{(k)} \hat{\Omega}^{(k)}, \quad (\hat{G}^{(k)})^* \hat{B}^{(k)} \hat{G}^{(k)} = I, \quad k = 0, 1, \dots, p-1,$$

where $\hat{B}^{(k)} = (\hat{Y}^{(k)})^* \hat{Y}^{(k)}$ and $\hat{\rho} = \sum_{k=0}^{p-1} \text{diag}[\hat{Y}^{(k)} \hat{G}^{(k)} (\hat{G}^{(k)})^* (\hat{Y}^{(k)})^*]$, each TRSCF iteration will loop over p unit cells and solve p linear generalized eigenvalue problems. The eigenvector matrices $\hat{G}^{(k)}$'s are used to update $\hat{\rho}$ before the next TRSCF begins. Typically, three to five TRSCF iterations are sufficient to reduce the total energy by a large factor within the subspace spanned by columns of $\hat{Y}^{(k)}$. There is no need to find the true minimizer of the subspace energy minimization problem when the subspace does not contain the solution to Kohn–Sham problem.

4. Numerical example

In this section, we will give an example that illustrates the convergence of the DCM algorithm when it is applied to a periodic system. The system we used in this example contains eight unit cells of a Gallium(Ga)/Arsenic(As) structure. Each unit cell contains four Ga atoms and four As atoms. The positions of these atoms are shown in Fig. 6. Each Ga atom has three valence electrons, and each As atom has five valence electrons. Thus the total number of valence electrons in the eight unit cell system is $n_e = 8 \cdot (4 \cdot 3 + 4 \cdot 5) = 256$. Each unit cell is cubic with the unit cell size $R = 10.6826$ Bohr. The Born–von Karman boundary condition is imposed in our calculation which implies that we use eight evenly spaced k -points in the first BZ $[0, 2\pi/R) \times [0, 2\pi/R) \times [0, 2\pi/R)$.

The Kohn–Sham minimization problem is discretized using a planewave discretization, i.e., each $\psi_i(r)$ is expressed as a linear combination of planewaves. The number of planewaves used in the expansion is $m = 13541$, which corresponds to a kinetic energy cutoff of 30 Rydberg. As we indicated at the end of Section 2, the use of planewave discretization does not alter the unit-cell decomposition property of the Kohn–Sham Hamiltonian shown in (23). The spectrum of the decoupled kinetic energy operator $T^{(k)}$ in a 3D version of (24) is different from (and more accurate than) that obtained from a finite difference discretization. However, both discretization schemes yield a $T^{(k)}$ that contains a k -dependent “phase factor”.

We use Troullier and Martins [15] ionic pseudopotentials in Kleinman and Bylander form to account for potential induced by Ga and As ionic cores. The preconditioner M that appears in (28) is chosen to be the kinetic energy operator T .

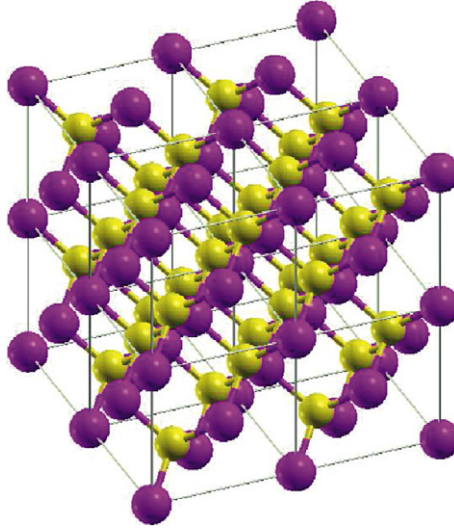


Fig. 6. A GaAs periodic system with eight unit cells. Each unit cell contains four Ga atoms and four As atoms.

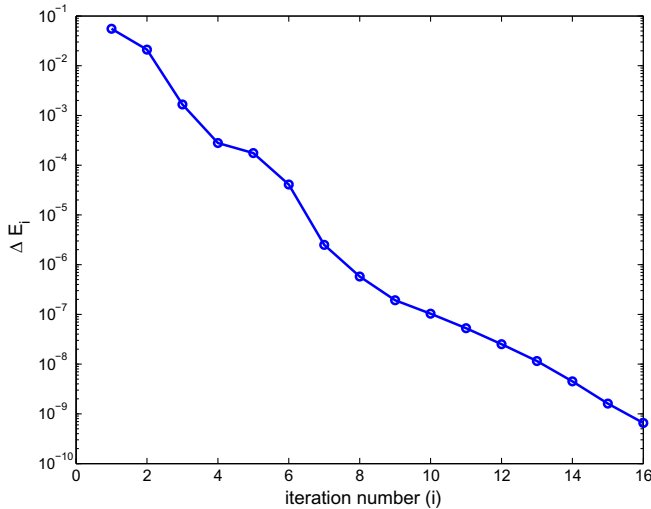


Fig. 7. The reduction in Kohn-Sham total energy in the DCM algorithm for the eight unit cell GaAs model.

Fig. 7 shows how the computed Kohn-Sham total energy changes in the DCM algorithm with respect to the iteration number. We plot $\Delta E_i = E_{ks}(X^{(i)}) - E_{min}$, where E_i is the total energy evaluated at the end of the i th DCM outer iteration, E_{min} is the minimum total energy obtained in a separate run. Three inner TRSCF iterations were used to solve the subspace minimization problem in Step 8 of the DCM algorithm. This figure shows that the computed total energy in DCM decreases monotonically at a rapid rate.

Appendix

Lemma 1. Suppose $d = F_n t$, where $t = (2 \ 1 \ 0 \ \cdots \ 0 \ -1)^T \in \mathbb{R}^n$, and F_n is the discrete Fourier transform matrix

$$F_n = \frac{1}{\sqrt{n}} \begin{pmatrix} 1 & 1 & 1 & \cdots & 1 \\ 1 & \omega_n & \omega_n^2 & \cdots & \omega_n^{n-1} \\ \vdots & \omega_n^2 & \omega_n^4 & \cdots & \omega_n^{2(n-1)} \\ \vdots & \vdots & \vdots & \cdots & \vdots \\ 1 & \omega_n^{n-1} & \omega_n^{2(n-1)} & \cdots & \omega_n^{(n-1)(n-1)} \end{pmatrix},$$

and $n = mp$ for some $m, p \in \mathbb{Z}^+$. If $d^{(k)}$, $k = 0, 1, \dots, p-1$, is obtained by sampling every p th element of d starting from the $k+1$ st element, then $d^{(k)}$ can be expressed by

$$d^{(k)} = F_m t^{(k)},$$

where $t^{(k)} = (2 \ \omega_n^k \ 0 \ \cdots \ 0 \ \omega_n^{-k})^T$.

Proof. The j th row of $d^{(k)}$ can be expressed by

$$\begin{aligned} e_j^T d^{(k)} &= e_j^T F_n t \\ &= \left(1 \ \omega_n^{(j-1)p+k} \ \omega_n^{2(j-1)p+2k} \ \cdots \ \omega_n^{(n-1)(j-1)p+(n-1)k} \right) \begin{pmatrix} 2 \\ -1 \\ 0 \\ \vdots \\ 0 \\ -1 \end{pmatrix} \\ &= \underbrace{\left(1 \ \omega_n^{(j-1)p} \ \omega_n^{2(j-1)p} \ \cdots \ \omega_n^{(n-1)(j-1)p+nk} \right)}_m \begin{pmatrix} 2 \\ -\omega_n^k \\ 0 \\ \vdots \\ 0 \\ -\omega_n^{-k} \end{pmatrix} \\ &= \left(1 \ \omega_m^{j-1} \ \omega_m^{2(j-1)} \ \cdots \ \omega_m^{(m-1)(j-1)} \right) t^{(k)}. \end{aligned} \tag{32}$$

Note that in (32), we reduced the lengths of both the row and column vectors to m , and modified elements 3 through $m-1$ in the row vector by setting them to $\omega_n^{2(j-1)p}$, $\omega_n^{3(j-1)p}$, ..., $\omega_n^{(n-2)(j-1)p}$. Such a modification does not change the product of these two vectors because the corresponding elements in the column vector are zeros. Since the vector $(1 \ \omega_m^{j-1} \ \omega_m^{2(j-1)} \ \cdots \ \omega_m^{(m-1)(j-1)})$ forms the j th row of F_m , for $j = 1, 2, \dots, m$, it follows that $d^{(k)} = F_m t^{(k)}$, and $n_e = sp$. \square

Acknowledgements

This work was supported by the Director, Office of Science, Division of Mathematical, Information, and Computational Sciences of the U.S. Department of Energy under Contract No. DE-AC02-05CH11231.

The computational results presented were obtained at the National Energy Research Scientific Computing Center (NERSC), which is supported by the Director, Office of Advanced Scientific Computing Research of the U.S. Department of Energy under Contract No. DE-AC02-05CH11232. The authors thank Byoungnak Lee and Lin-Wang Wang for helpful discussions. The authors also thank anonymous referees for careful reading and helpful suggestions.

References

- [1] W. Kohn, L.J. Sham, *Phys. Rev.* 140 (1965) A1133–A1138.
- [2] E. Kaxiras, *Atomic and Electronic Structure of Solids*, Cambridge University Press, 2003.
- [3] J.C. Phillips, *Phys. Rev.* 112 (1958) 685–695.
- [4] J.C. Phillips, L. Kleinman, *Phys. Rev.* 116 (1958) 287–294.
- [5] M.T. Yin, M.L. Cohen, *Phys. Rev. B* 25 (1982) 7403–7412.
- [6] F. Nogueira, A. Castro, M. Marques, *A Primer in Density Functional Theory*, Springer, Berlin, 2003, pp. 218–256.
- [7] F. Bloch, *Z. Phys.* 52 (1928) 555.
- [8] N.W. Ashcroft, N.D. Mermin, *Solid State Physics*, Brooks Cole, Pacific Grove, CA, 1976.
- [9] M. Reed, B. Simon, *Methods of Modern Mathematical Physics. IV: Analysis of Operators*, Academic Press, 1978.
- [10] C. Yang, J.C. Meza, L.W. Wang, *J. Comput. Phys.* 217 (2005) 709–721.
- [11] P.J. Davis, *Circulant Matrices*, Wiley, New York, 1979.
- [12] F. Weinhold, C.R. Landis, *Valency and Bonding: A Natural Bond Orbital Donor–Acceptor Perspective*, Cambridge University Press, 2005.
- [13] H.J. Monkhorst, J.D. Pack, *Phys. Rev. B* 13 (1976) 5188–5192.
- [14] C. Yang, J.C. Meza, L.W. Wang, *SIAM J. Sci. Comput.* 29 (2007) 1854–1875.
- [15] N. Troullier, J.L. Martins, *Phys. Rev. B* 43 (1991) 1993–2005.